

## MODEL ORDER REDUCTION FOR PEEC MODELING BASED ON MOMENT MATCHING

**Z. F. Song and D. L. Su**

EMC Laboratory, Beihang University  
37 XueYuan Road, Haidian District, Beijing 100191, China

**F. Duval and A. Louis**

IRSEEM/ESIGELEC  
Technôpole du Madrillet, Avenue Galilée, BP 10024  
Saint Etienne du Rouvray 76801, France

**Abstract**—Accurate and effective system-level modeling has become necessary to address electromagnetic compatibility (EMC) issues in modern circuit and system design. Model order reduction (MOR) techniques provide a feasibility to approximate complex circuit models with compact reduced-order models. In this paper, an effective MOR technique entitled multi-point moment matching (MMM) is implemented for the partial element equivalent circuit (PEEC) modeling. Moment information at multiple frequency points is used in this method in order to accurately estimate a given system over an entire frequency range of interest, and for each frequency an enhanced asymptotic waveform evaluation (AWE) is applied to obtain a reduced-order model by constructing a pole-residue representation of the original transfer function. The improvements of conventional AWE in aspects of both moment computation and moment matching can avoid ill-conditioned moment matrices and unstable dominant poles. The complex frequency hopping (CFH) technique is employed to select the multiple expansion points by using a newly developed upward-search algorithm. Numerical simulations of coupled microstrip lines in both frequency and time domain indicate the effectiveness of the proposed method.

## 1. INTRODUCTION

The increasing complexities of physical structures, signal features and electromagnetic (EM) environment of modern electronic systems make EM modeling an increasingly tough task. Despite significant advances in EM modeling methodologies, computational efficiency is desirable especially for complex modeling problems.

Currently, the partial element equivalent circuit (PEEC) method [1] is one of the promising numerical methods for EM modeling of various engineering problems, e.g., EM compatibility (EMC), EM interference (EMI), and signal integrity (SI) of high-speed digital circuits [2]. The main advantage of PEEC is its ability to provide a circuit interpretation of the electric field integral equation (EFIE) in terms of partial elements, namely resistances, partial inductances and coefficients of potential. It especially has great potentials for mixed electromagnetic-circuit problems because it is ease to integrate the field solver with real circuit elements.

Integration of a PEEC model directly into a circuit simulator is computationally expensive for two main facts. One is that a large number of circuit elements are generated for complex structures at high frequencies; and the other is that the circuit matrices based on modified nodal analysis (MNA) [3] are usually dense due to full inductive and capacitive coupling. In order to model/simulate such problems efficiently, developing compact model representation via model order reduction (MOR) [4, 5] is desirable for PEEC modeling.

The basic idea of MOR techniques is to reduce the size of a system described by circuit equations, but preserve the dominant behavior of the original system. MOR techniques, for instance, the asymptotic waveform evaluation (AWE) [6–8], Krylov subspace projection based algorithms (e.g., Lanczos method [9–11], Arnoldi algorithm [12, 13], and passivity-preserving PRIMA [14, 15]), and truncated balanced realization (TBR) methods [15] have been topics of intense research in the EM modeling field in recent years.

AWE is an efficient approximation either in frequency domain or time domain where explicit moment matching is employed to compute the dominant poles and residues of the order truncated transfer functions via the Padé approximation. In various practical applications, it was found that AWE suffers from ill-conditioned moment matrices especially for the higher-order moment approximation [4]. In addition, since a Padé approximation is accurate only near the expansion point, AWE is limited in its ability to capture the dominant poles of a network over a wide frequency range [17]. To achieve accurate simulations in various EM modeling applications,

a more effective method proposed in this paper uses a multi-point moment matching (MMM) technique. Moment information at multiple expansions is employed in this method. For moment matching at each expansion point, the approximation is improved by combining several procedures. The moment computation for each expansion is enhanced by the moment scaling and frequency shifting; meanwhile the accurate dominant poles can be obtained by moment shifting. Complex frequency hopping (CFH) [18] is employed where an efficient upward-search strategy is incorporated for the selection and minimization expansion points over the frequency bandwidth of interest. Numerical experiments show that the proposed multi-point moment matching is suitable for PEEC modeling when no external nonlinear circuit elements are connected.

This paper is organized as follows. An overview of PEEC formulations using MNA is proposed in Section 2. The framework of PEEC modeling based on model order reduction techniques is presented in Section 3, and the proposed MMM based reduced-order modeling is detailed in this section as well. Section 4 gives a modeling example of coupled microstrip lines. Finally, Section 5 ends with conclusions.

## 2. PEEC FORMULATION

The basic full-wave PEEC formulation is derived from the electric field integral equation which is given by

$$\mathbf{E}^i(\mathbf{r}, t) = \frac{\mathbf{J}(\mathbf{r}, t)}{\sigma} + \mu \frac{\partial}{\partial t} \int G(\mathbf{r}, t, \mathbf{r}', t') \mathbf{J}(\mathbf{r}', t') d^3\mathbf{r}' dt' + \frac{1}{\varepsilon} \nabla \int G(\mathbf{r}, t, \mathbf{r}', t') \rho(\mathbf{r}', t') d^3\mathbf{r}' dt'; \quad (1)$$

where  $\mathbf{E}^i$  denotes the incident electric field, and the unknowns,  $\mathbf{J}$  and  $\rho$  are the current density in the interior and the charge density on the surface of the conductors, respectively.  $\sigma$  is the conductivity of the conductor; and  $\mu$  and  $\varepsilon$  represent the permeability and the permittivity in the surrounding medium, respectively.

The corresponding Green's function in (1) is given by

$$G(\mathbf{r}, t, \mathbf{r}', t') = \frac{\delta(t - t' - |\mathbf{r} - \mathbf{r}'|/c)}{4\pi|\mathbf{r} - \mathbf{r}'|}; \quad (2)$$

where the Dirac delta function in the numerator is the result of the finite value of the speed of light in the background medium,  $c = 1/\sqrt{\mu\varepsilon}$ , which causes a time delay.

The PEEC model also includes the continuity equation  $\nabla \cdot \mathbf{J} + \frac{\partial}{\partial t} \rho = 0$  as the Kirchoff's current law at each node of equivalent circuits. The EFIE and continuity equation are spatially discretized using the *Galerkin method*, where a current basis function  $\Psi_i(\mathbf{r})$  and a charge basis function  $\Phi_s(\mathbf{r})$  are introduced.

$$\mathbf{J}(\mathbf{r}, t) = \sum_{i=1}^{N_v} I_i(t) \Psi_i(\mathbf{r}). \quad (3)$$

$$\rho(\mathbf{r}, t) = \sum_{s=1}^{N_s} Q_s(t) \Phi_s(\mathbf{r}). \quad (4)$$

The volume current density and surface charge density can be described as (3) and (4), where  $N_v$  and  $N_s$  are the numbers of volume and surface discretization respectively. The most popular choice of the basis functions is piecewise constant basis functions. The information of cross sections of volume-cells is included in the current basis function  $\Psi_i(\mathbf{r})$ , and  $\Phi_s(\mathbf{r})$  contains the information of surface area of surface-cells. The discretization procedure implies that the current density flows through each volume-cell and the surface charge density on each surface-cell are considered as constants.

To interpret the field relation as equivalent circuit equations, the partial circuit elements are defined. The Equations (5) and (6) give the definitions of partial inductance and partial coefficient of potential respectively. Equation (7) is the resistance of a volume-cell.

$$L_{ij}(t, t') = \mu \iint \Psi_i(\mathbf{r}) G(\mathbf{r}, t, \mathbf{r}', t') \Psi_j(\mathbf{r}') d^3 \mathbf{r}' d^3 \mathbf{r}; \quad (5)$$

$$P_{ml}(t, t') = \frac{1}{\varepsilon} \iint \Phi_m(\mathbf{r}) G(\mathbf{r}, t, \mathbf{r}', t') \Phi_l(\mathbf{r}') d^3 \mathbf{r}' d^3 \mathbf{r}; \quad (6)$$

$$R_{ij} = \int \Psi_i(\mathbf{r}) \frac{1}{\sigma(\mathbf{r})} \Psi_j(\mathbf{r}) d^3 \mathbf{r}. \quad (7)$$

Since  $\mathbf{J}$  and  $\rho$  and are coupled by the continuity equation, it is natural to match the current and charge basis functions, in the sense that each current basis function takes charge from one charge basis function to another [16]. In other words,

$$\nabla \cdot \Psi_i = \sum_{s=1}^{N_s} E_{is} \Phi_s. \quad (8)$$

The matrix  $E$  is a sparse  $N_v \times N_s$  matrix and its entry is defined as

$$E_{is} = \begin{cases} +1 & \text{if } \Psi_i \text{ takes charges from } \Phi_s \\ -1 & \text{if } \Psi_i \text{ puts charges to } \Phi_s \\ 0 & \text{remaining parts} \end{cases}.$$

The EFIE (1) and continuity equation can be rewritten as a group of matrix differential equations.

$$\begin{cases} L\dot{I} - EPQ + RI = 0 \\ E^T I + \dot{Q} = 0 \end{cases} \quad (9)$$

The electrostatic potential at each surface-cell is given by  $V = PQ$ , which will be the node voltages in the equivalent circuit. So we can write the PEEC formulation in MNA matrix circuit equations

$$\begin{cases} C\dot{x}(t) + Gx(t) = bu(t) \\ y(t) = l^T x(t) \end{cases}, \quad (10)$$

where:  $C = \begin{bmatrix} L & 0 \\ 0 & P^{-1} \end{bmatrix}$ ;  $G = \begin{bmatrix} R & -E \\ E^T & 0 \end{bmatrix}$ ;  $x(t) = \begin{bmatrix} I \\ V \end{bmatrix}$ .

The vectors  $u(t)$  and  $y(t)$  denote excited sources and port outputs, respectively.  $b$  and  $l$  are selector matrices. The state parameter  $x(t)$  is composed of  $I$  and  $V$  which are the MNA variables corresponding to the branch currents and node voltages.

### 3. REDUCED ORDER MODELING BASED ON MOMENT MATCHING

Figure 1 illustrates the working flow of the proposed reduced-order PEEC modeling. As conventional solutions, the equivalent circuit of a parameterized modeling structure can be generated with the conventional PEEC discretization. The circuit description based on MNA is created after completing the calculation of partial element matrices.

A multi-point moment matching (MMM) technique is employed to approximate the transfer function of an original system using moment information at multiple frequency points, and an enhanced single-point moment matching technique is used at each expansion point. Ill-conditioned moment matrices and unstable dominant poles in conventional AWE may result in inaccurate responses. In order to overcome this problem, the moment computation for each frequency point expansion is enhanced by combining the moment scaling and frequency shifting techniques; meanwhile the accurate dominant poles can be obtained by moment shifting. In the proposed MMM procedure, we adopt the complex frequency hopping, where an adaptive upward-search strategy is incorporated for selecting and minimizing expansion points over the frequency bandwidth of interest.

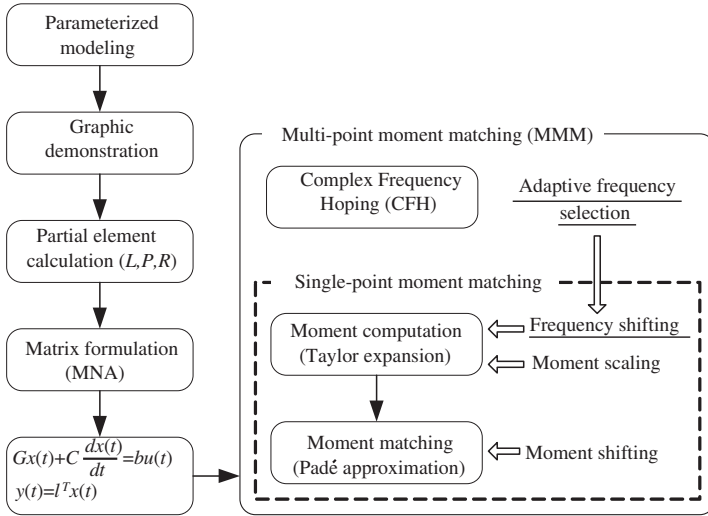


**Figure 1.** Flowchart of the reduced-order PEEC modeling.

### 3.1. Single-point Moment Matching

Applying the Laplace transform of the MNA formulation (10), we can obtain corresponding state equations in  $s$  domain. Under the assumption of an initial condition  $X(0) = 0$ , the transfer function  $H(s)$  from input  $U(s)$  to output  $Y(s)$  is given by

$$H(s) = \frac{Y(s)}{U(s)} = l^T (G + sC)^{-1} b. \tag{11}$$

The AWE in general consists of two stages, i.e., moment computation and moment matching. Specifically, the moments are the coefficients of an expansion of the transfer function [5].

$$H(s) = l^T [I + sG^{-1}C]^{-1} G^{-1} b = \sum_{i=0}^{\infty} m_i (s - s_0)^i. \tag{12}$$

The moments  $m_i$  can be computed as

$$m_i = l^T A^i r, \tag{13}$$

where  $A = -(G + s_0 C)^{-1} C$ ,  $r = (G + s_0 C)^{-1} b$ .

Moment matching finds an order-limited rational function representation  $\tilde{H}(s)$  for the original transfer function  $H(s)$  using Padé approximation. The general  $[L/M]$  type Padé approximation has a

form of (14), where  $L$  and  $M$  denote the orders of the numerator and denominator, respectively.

$$\tilde{H}(s) = \frac{P^L(s)}{Q^M(s)} = \frac{\sum_{i=0}^L a_i(s - s_0)^i}{1 + \sum_{j=1}^M b_j(s - s_0)^j}. \tag{14}$$

A set of  $2M$  successive moments  $\{m_{L-M+1}, m_{L-M+2}, \dots, m_{L+M}\}$  will be used to calculate the coefficients of the denominator polynomial in (14) according to the linear equation

$$\begin{bmatrix} m_{L-M+1} & m_{L-M+2} & \cdots & m_L \\ m_{L-M+2} & m_{L-M+3} & \cdots & m_{L+1} \\ \vdots & \vdots & \ddots & \vdots \\ m_L & m_{L+1} & \cdots & m_{L+M-1} \end{bmatrix} \begin{bmatrix} b_M \\ b_{M-1} \\ \vdots \\ b_1 \end{bmatrix} = - \begin{bmatrix} m_{L+1} \\ m_{L+2} \\ \vdots \\ m_{L+M} \end{bmatrix}. \tag{15}$$

Alternatively, poles and residues give a partial fraction representation of the rational transfer function  $\tilde{H}(s)$  in a form of

$$\tilde{H}(s') = \frac{P^L(s')}{Q^M(s')} = \sum_{i=1}^M \frac{k_i}{s' - p_i}, \tag{16}$$

here  $s' = s - s_0$ , and  $k_i$ 's,  $p_i$ 's are residues and poles, respectively.

The poles are actually the roots of the denominator polynomial  $Q^M(s')$ , and the respective residues can be calculated by

$$\begin{bmatrix} p_1^{-1} & p_2^{-1} & \cdots & p_q^{-1} \\ p_1^{-2} & p_2^{-2} & \cdots & p_q^{-2} \\ \vdots & \vdots & \ddots & \vdots \\ p_1^{-q} & p_2^{-q} & \cdots & p_q^{-q} \end{bmatrix} \begin{bmatrix} k_1 \\ k_2 \\ \vdots \\ k_q \end{bmatrix} = - \begin{bmatrix} m_0 \\ m_1 \\ \vdots \\ m_{q-1} \end{bmatrix}. \tag{17}$$

With the pole-residue representation of the transfer function, it is easy to estimate system responses in frequency domain by

$$Y(s) = \tilde{H}(s) \cdot U(s). \tag{18}$$

Time domain response can be approximated indirectly through Laplace transform and inverse Laplace transform as

$$y(t) = \mathcal{L}^{-1} \left\{ \tilde{H}(s) \cdot \mathcal{L}\{u(t)\} \right\}; \tag{19}$$

here  $\mathcal{L}\{\cdot\}$  and  $\mathcal{L}^{-1}\{\cdot\}$  denote the operators of Laplace transform and inverse Laplace transform.

We take a unit ramp input  $r(t)$  as an example. The Laplace transform of the input is  $\mathcal{L}\{r(t)\} = 1/s^2$ ; therefore, the corresponding transient response obtained by (19) can be written as

$$y_r(t) = \left[ \sum_{i=1}^q \frac{k_i}{p_i^2} (e^{p_i t} - p_i r(t) - 1) \right] u(t); \tag{20}$$

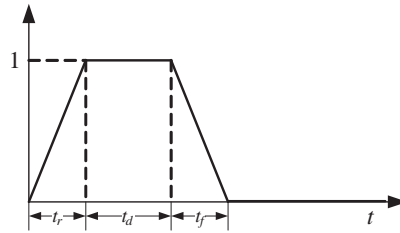


**Figure 2.** A pulse input waveform.

where  $u(t)$  is a unit step function.

This approach of the time-domain response calculation can be extended to general inputs by applying superposition of elementary responses. A pulse input which is widely used in the interconnect analysis is shown in Fig. 2. The input waveform can be expressed as (21), and the corresponding time-domain response is given by (22).

$$V_{input}(t) = \frac{1}{t_r} [r(t) - r(t - t_r)] - \frac{1}{t_f} [r(t - t_r - t_d) - r(t - t_r - t_d - t_f)]. \quad (21)$$

$$V_{output}(t) = \frac{1}{t_r} [y_r(t) - y_r(t - t_r)] - \frac{1}{t_f} [y_r(t - t_r - t_d) - y_r(t - t_r - t_d - t_f)], \quad (22)$$

here  $y_r(t)$  is the response of a unit ramp input which is shown in (20).

### 3.2. Enhanced AWE

The performance of AWE depends on the invertibility and condition number of the corresponding moment matrix in (15) [17]. The moment matrix easily becomes increasingly ill-conditioned or near singular as its size increases. This implies that higher order approximation is impossible and thus one can only expect to extract only a few accurate poles from a single expansion. The condition of the moment matrix can be improved by scaling the moment values. One can refer to [17, 18] for the detail of the moment scaling technique.

The approximation will lose its accuracy with increasing distances in complex  $s$  plane from the expansion point. Conventional (standard) AWE uses the moments expanded at the origin, so it is not sufficient for high frequency approximations. The frequency shifting technique uses Taylor's expansion at frequency point  $s_0$  ( $s_0 \neq 0$ ) for the moment calculation, and  $s' = s - s_0$  can still preserve the usage of standard AWE.

An entire matrix of possible Padé approximations with respect to different choices of  $L$  and  $M$  is known as Padé table. One of the

important properties of Padé approximation is that poles of horizontal sequences (fixed  $M$ , increasing  $L$ ) in the table converge to the actual poles [18, 19]. This is as (23) indicates, where  $p_j$ 's are the actual poles of transfer function. Based on this property, a method entitled moment shifting is utilized to obtain accurate poles. The basic idea of this improvement is to use higher order moments in horizontal sequences to obtain stable poles. The corresponding residues can be obtained by (17) as usual once the stable poles are found.

$$\lim_{L \rightarrow \infty} Q^M(s) = \prod_{j=1}^M \left( 1 - \frac{s}{p_j} \right). \quad (23)$$

### 3.3. Multi-point Moment Matching

The CFH extends the conventional single-point moment matching to an efficient multi-point moment matching. The moments at multiple expansions are obtained to enable an approximate transfer function which matches the original function up to a predefined highest frequency of interest [20].

In CFH, at least two expansion points are required. The accuracy of any two successive expansions can be checked by matching the poles generated at these points [18]. Alternatively, the successive expansions can be also verified for their accuracy by comparing values of the approximate transfer functions obtained at these expansions with respect to a point intermediate to them [21, 22]. The former two-point selection criterion is incorporated in the proposed approach.

CFH relies on the specific search algorithm to determine the expansion points and to minimize the number of expansions over the entire frequency bandwidth. The specific search algorithm involved in our research can be referred as an *upward-search approach* illustrated in Fig. 3. The expansion points are chosen in the complex plane near or on the imaginary axis. High frequency response is dominated by higher order moments and thus a denser expansion point selection should be adopted at higher frequency range. From this point of view, the proposed upward-search is developed to obtain a non-uniform expansion selection. The steps involved in the search approach are summarized as follows:

```

 $f_L = f_{\min};$ 
 $f_H = f_{\max};$ 
while  $f_H$  % endless loop with only one exit
    if  $CFH_{conv}(f_L, f_H) = true$ 
        break; % the only loop exit of the search process
        record pole-residues at  $f_L$  and  $f_H$ ;

```

```

else
    while  $CFH\_conv(f_L, f_H) = false$ 
         $f_L = \frac{1}{2}(f_L + f_H)$ 
    end
    record pole-residues at  $f_H$  and  $f_H$ ;
     $f_H = f_L$ ;
     $f_L = f_{min}$ ;
end
end
record pole-residues at  $f_L$  and  $f_L$ ;

```

The  $CFH\_conv(f_L, f_H)$  in the above MATLAB code flow denotes the two-point selection criterion for  $f_L$  and  $f_H$ , and its true value implies that the moment information at  $f_L$  and  $f_H$  is sufficient for moment matching in the frequency range  $f_L \sim f_H$ .

The whole process starts with the boundary frequencies of the investigated bandwidth,  $f_{min}$  and  $f_{max}$ . Firstly, one determines the two-point selection criterion by  $CFH\_conv(f_{min}, f_{max})$ . The search stops subject to the satisfaction of the selection criterion; otherwise continue the search by determining  $CFH\_conv(f_1^{(1)}, f_{max})$ , here  $f_1^{(1)} = \frac{1}{2}(f_{min} + f_{max})$ . The notation  $f_i^{(k)}$  denotes the  $i$ th interpolated expansion point between  $f_{min}$  and  $f_{max}$  after  $k$  determination loops. Following such procedure, the sub-process stops only if the two-point selection criterion is satisfied at a point  $f_1^{(k+1)}$  (intermediate to  $f_{max}$  and the previous point  $f_1^{(k)}$ ) and  $f_{max}$ . In the case illustrated in Fig. 3, the first two expansions after three rounds of tests are  $f_1^{(3)}$  and  $f_{max}$ .

Secondly, a similar process is employed at the left part of frequency band ( $f_{min} \sim f_1^{(3)}$ ). The final determined expansion points in Fig. 3 are  $f_{min}$ ,  $f_3^{(1)}$ ,  $f_2^{(2)}$ ,  $f_1^{(3)}$  and  $f_{max}$ . Due to the search trend towards the upper boundary in the process, a name of upward-searching is given.

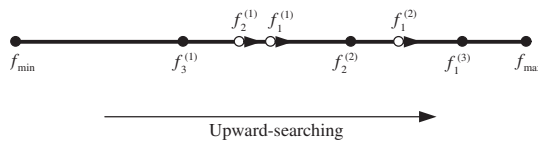


**Figure 3.** An upward-searching algorithm for expansion point selection.

#### 4. NUMERICAL RESULTS

The configuration of coupled microstrip lines shown in Fig. 4 is typical in printed circuit board (PCB) structures. The common ground provides a possibility of interference due to crosstalk. The two transmission conductors are 50 mm long and 3 mm apart. They have identical rectangular cross sections with dimensions of 1 mm in width and 0.2 mm in thickness. A voltage excitation source,  $V_S$  (1 volt) consisting of a source resistance  $R_S$  (50 ohms) is connected at a terminal  $S$ , and another end of the generator conductor is terminated with a 50 ohms resistor. A receptor conductor connects two terminations  $NE$  and  $FE$ , represented by resistors  $R_{NE}$  (50 ohms) and  $R_{FE}$  (50 ohms).

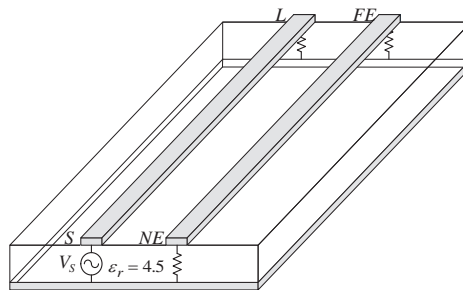


**Figure 4.** A simulation structure of coupled microstrip lines.

The basic rule of thumb for surface- and volume-cell discretization in PEEC modeling is to use a fixed number of cells per shortest wavelength  $\lambda_{\min}$  (corresponding to the highest frequency of interest).  $20 \text{ cells}/\lambda_{\min}$  is considered in this PEEC model. The full PEEC model is solved using conventional spice-solvers, e.g., Pspice. The corresponding reduced-order model can be obtained from the MNA formulation and solved by moment matching.

The induced voltages from 1 MHz and up to 5 GHz at the near end  $NE$  are investigated. Fig. 5 shows the frequency responses obtained by spice-solver, single-point moment matching, i.e., standard AWE and MMM. Good agreements of Pspice results and MMM results are obtained, while the conventional AWE fails beyond 1 GHz. Table 1 also shows numbers of expansion points with respect to frequency ranges. Normally, more expansion points are necessary for a wider frequency range. Comparing with total investigated frequency points (e.g., 30 points/decade in this case), the upward-search algorithm is computationally effective.

In addition, for transient response analysis, the terminal  $S$  is

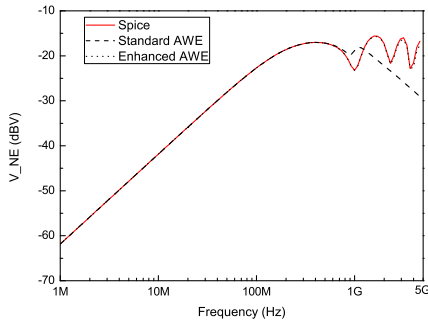


**Figure 5.** Frequency domain (1 MHz  $\sim$  5 GHz) responses at the near end.

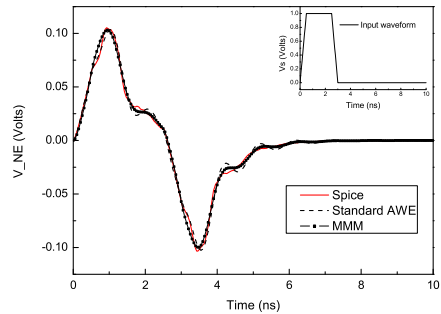


**Figure 6.** Time domain responses at the near end.

**Table 1.** Numbers of expansion points with respect to frequency ranges.

Frequency range	Number of points
1 MHz $\sim$ 100 MHz	2
1 MHz $\sim$ 500 MHz	9
1 MHz $\sim$ 1 GHz	11
1 MHz $\sim$ 5 GHz	20

excited by a voltage pulse with 0.5 ns rise/fall time and 2 ns duration. The voltage waveform induced at near-end  $NE$  has been computed by using both spice-solver and reduced-order modeling. The results are shown in Fig. 6. Comparing the results by conventional AWE and the proposed MMM method, better agreements with Pspice results are obtained by using MMM.

## 5. CONCLUSION

The MNA approach provides PEEC models with systemic linear state-space matrix formulation description, which offers a possibility of reduced-order modeling. In this paper, an effective model order reduction technique based on multi-point moment matching is proposed to improve the PEEC modeling. Efficient approximations can be achieved in a local expansion point by a single-point moment matching, i.e., AWE; nevertheless, conventional AWE suffers from ill-conditioned moment matrices and unstable dominant poles which result in inaccurate responses. The proposed enhanced AWE combines

some improvements in aspects of both moment computation and moment matching to overcome these problems. To effectively represent a system over a wide frequency range, moment information at multiple expansions is used in the proposed MMM method. An upward-search algorithm assembled in the CFH technique is employed to select the multiple expansion points. It can be concluded from the numerical simulations that PEEC method in conjunction with the proposed reduced-order modeling procedure has extensive applications.

## ACKNOWLEDGMENT

The authors would like to thank China Scholarship Council (CSC) for offering the first author an precious research opportunity in France.

## REFERENCES

1. Ruehli, A. E., "Equivalent circuit models for three dimensional multiconductor systems," *IEEE Trans. on Microwave Theory and Tech.*, Vol. 22, No. 3, 216–221, Mar. 1974.
2. Ruehli, A. E. and A. C. Cangellaris, "Progress in the methodologies for the electrical modeling of interconnects and electronic packages," *Proc. IEEE*, Vol. 89, No. 5, 740–771, May 2001.
3. Ho, C., A. E. Ruehli, and P. Brennan, "The modified nodal approach to network analysis," *IEEE Trans. Circuits Syst.*, Vol. 22, No. 6, 504–509, Jun. 1975.
4. Tan, S. X. D. and L. He, *Advanced Model Order Reduction Techniques in VLSI Design*, Cambridge University Press, Cambridge, 2007.
5. Zhu, Y. and A. C. Cangellaris, *Multigrid Finite Element Methods for Electromagnetic Field Modeling*, John Wiley & Sons Inc., Hoboken, New Jersey, 2006.
6. Pillage, L. T. and R. A. Rohrer, "Asymptotic waveform evaluation for timing analysis," *IEEE Trans. Comput. — Aided Des.*, Vol. 9, No. 4, 352–366, Apr. 1990.
7. Liu, P., Z. F. Li, and G. B. Han, "Application of asymptotic waveform evaluation to eigenmode expansion method for analysis of simultaneous switching noise in printed circuit boards (PCBs)," *IEEE Trans. Electromagn. Compat.*, Vol. 48, No. 3, 485–492, Aug. 2006.
8. Wan, J. X. and C.-H. Liang, "Rapid solutions of scattering from microstrip antennas using well-conditioned asymptotic waveform

- evaluation,” *Progress In Electromagnetics Research*, Vol. 49, 39–52, 2004.
9. Feldman, P. and R. W. Freund, “Efficient linear circuit analysis by Pade approximation via a Lanczos method,” *IEEE Trans. Comput. — Aided Des.*, Vol. 14, No. 5, 639–649, May 1995.
  10. Carpentieri, B., Y. F. Jing, and T. Z. Huang, “A novel Lanczos-type procedure for computing eigenelements of Maxwell and Helmholtz problems,” *Progress In Electromagnetics Research*, Vol. 110, 81–101, 2010.
  11. Remis, R. F., “An efficient model-order reduction approach to low-frequency transmission line modeling,” *Progress In Electromagnetics Research*, Vol. 101, 139–155, 2010.
  12. Zhang, Z. and Y. H. Lee, “An automatic model order reduction of a UWB antenna system,” *Progress In Electromagnetics Research*, Vol. 104, 267–282, 2010.
  13. Lancellotti, V., B. P. de Hon, and A. G. Tijhuis, “Scattering from large 3-d piecewise homogeneous bodies through linear embedding via green’s operators and arnoldi basis functions,” *Progress In Electromagnetics Research*, Vol. 103, 305–322, 2010.
  14. Odabasioglu, A., M. Celik, and L. T. Pileggi, “PRIMA: Passive reduced-order interconnect macromodeling algorithm,” *IEEE Trans. Comput. — Aided Des. Integr. Syst.*, Vol. 17, No. 8, 645–654, Aug. 1998.
  15. Steinmair, G. and R. Weigel, “Analysis of power distribution systems on PCB level via reduced PEEC-modeling,” *15th Int. Conf. Microw. Radar and Wireless Commun., MIKON-2004*, Vol. 1, 283–286, Warszawa, Poland, May 2004.
  16. Verbeek, M. E., “Partial Element Equivalent Circuit (PEEC) models for on-chip passives and interconnects,” *Int. J. Numer. Model.*, Vol. 17, No. 1, 61–84, Feb. 2004.
  17. Celik, M., T. Pileggi, and A. Odabasioglu, *IC Interconnect Analysis*, Kluwer Academic Publishers, Dordrecht, 2002.
  18. Chiprout, E. and M. S. Nakhla, “Analysis of interconnect networks using complex frequency hopping (CFH),” *IEEE Trans. Comput. — Aided Des. Integr. Syst.*, Vol. 14, No. 2, 186–200, Feb. 1995.
  19. Anastasakis, D. F., N. Gopal, S. Kim, and L. T. Pillage, “Enhancing the stability of asymptotic waveform evaluation for digital interconnect circuit applications,” *IEEE Trans. Comput. — Aided Des. Integr. Syst.*, Vol. 13, No. 6, 729–736, Jun. 1994.
  20. Achar, R. and M. S. Nakhla, “Simulation of high-speed interconnects,” *Proc. IEEE*, Vol. 89, No. 5, 693–728, May 2001.

21. Sannaie, R., E. Chiprout, M. Nakhla, and Q. J. Zhang, "A fast method for frequency and time domain simulation of high-speed VLSI interconnects," *IEEE Trans. Microwave Theory Tech.*, Vol. 42, No. 12, 2562–2571, Dec. 1994.
22. Achar, R., M. S. Nakhla, and Q. J. Zhang, "Full-wave analysis of high-speed interconnects using complex frequency hopping," *IEEE Trans. Comput. — Aided Des. Integr. Syst.*, Vol. 17, No. 10, 997–1016, Oct. 1998.